

In vivo delivery of synthetic DNA-encoded antibodies induces broad HIV-1-neutralizing activity

Megan C. Wise,¹ Ziyang Xu,^{2,3} Edgar Tello-Ruiz,² Charles Beck,⁴ Aspen Trautz,² Ami Patel,² Sarah T.C. Elliott,² Neethu Chokkalingam,² Sophie Kim,² Melissa G. Kerkau,⁴ Kar Muthumani,² Jingjing Jiang,¹ Paul D. Fisher,¹ Stephany J. Ramos,¹ Trevor R.F. Smith,¹ Janess Mendoza,¹ Kate E. Broderick,¹ David C. Montefiori,⁵ Guido Ferrari,⁴ Daniel W. Kulp,² Laurent M. Humeau,¹ and David B. Weiner²

¹Inovio Pharmaceuticals, Plymouth Meeting, Pennsylvania, USA. ²Vaccine and Immunotherapy Center, The Wistar Institute, Philadelphia, Pennsylvania, USA. ³Perelman School of Medicine, University of Pennsylvania, Philadelphia, Pennsylvania, USA. ⁴Duke Human Vaccine Institute and ⁵Department of Surgery, Duke University School of Medicine, Durham, North Carolina, USA.

Interventions to prevent HIV-1 infection and alternative tools in HIV cure therapy remain pressing goals. Recently, numerous broadly neutralizing HIV-1 monoclonal antibodies (bNAbs) have been developed that possess the characteristics necessary for potential prophylactic or therapeutic approaches. However, formulation complexities, especially for multiantibody deliveries, long infusion times, and production issues could limit the use of these bNAbs when deployed, globally affecting their potential application. Here, we describe an approach utilizing synthetic DNA-encoded monoclonal antibodies (dmAbs) for direct in vivo production of prespecified neutralizing activity. We designed 16 different bNAbs as dmAb cassettes and studied their activity in small and large animals. Sera from animals administered dmAbs neutralized multiple HIV-1 isolates with activity similar to that of their parental recombinant mAbs. Delivery of multiple dmAbs to a single animal led to increased neutralization breadth. Two dmAbs, PGDM1400 and PGT121, were advanced into nonhuman primates for study. High peak-circulating levels (between 6 and 34 $\mu\text{g/ml}$) of these dmAbs were measured, and the sera of all animals displayed broad neutralizing activity. The dmAb approach provides an important local delivery platform for the in vivo generation of HIV-1 bNAbs and for other infectious disease antibodies.

Introduction

In just over four decades since its global emergence, the AIDS epidemic has taken millions of lives. While there have been exceptional advances in antiretroviral therapies, there remains a need for preventive treatments and interventions to eliminate HIV-1 infection (1). In recent years, multiple mAbs with potent neutralization capacity have been isolated from HIV-1-infected persons (2, 3). A few of these broadly neutralizing HIV-1 mAbs (bNAbs) have demonstrated efficacy in preventing infection after a single dose of intravenous recombinant protein in nonhuman primates (NHPs) (4). Such observations have generated enthusiasm in the field and progressed HIV-1 bNAbs into the clinic for studies of prevention (ClinicalTrials.gov NCT02256631, NCT02568215, NCT02716675) as well as for HIV treatment toward cure strategies (5–9). Recently, clinical trials have

explored the capability of these antibodies to lower viral loads or prevent rebound after analytical treatment interruption (ATI) (8, 9). Most notably, a study by Mendoza et al. demonstrated that a combination of 2 bNAbs, 3BNC117 and 10-1074, prevented viral rebound for a median of 21 weeks in a subset of individuals compared with 2.3 weeks in historical controls (6).

The widespread use of passive delivery of recombinant antibodies is affected due to infusion time, formulation issues, product temperature stability, redosing requirements, and substantial manufacturing costs (10). Viral vector delivery with adeno-associated virus (AAV) has been previously evaluated as a delivery platform for HIV-1 bNAbs, with high-level and long-term expression of the transgene antibody (11–13). However, AAV delivery can be limited in populations by preexisting neutralizing antibodies to the vector, safety concerns of permanent gene marking of the patient, temperature stability, and manufacturing cost as well as vector seroconversion potentially preventing readministration, ultimately resulting in reduced antibody levels in many subjects (14). Recent clinical results of recombinant AAV-1-delivered PG9 demonstrated limited detection of circulating PG9 in healthy males who were delivered a range of vector doses (4×10^{12} to 1.2×10^{14} vector genomes) (15). In this study, we explored the use of synthetic DNA-encoded mAbs (dmAbs) as a possible alternative, serology-independent approach to passive transfer and AAV delivery. Upon injection and electroporation of optimized plasmid DNA with transgenes encoding antibody, locally transfected cells become the in vivo biofactory for antibody production. We have previously demonstrated that this dmAb technology was able to

Authorship note: MCW and ZX contributed equally to this work.

Conflict of interest: MCW, JJ, PF, SJR, TRFS, JM, KEB, and LH are employees of Inovio Pharmaceuticals and, as such, receive salary and benefits, including ownership of stock and stock options. KM receives grants and consulting fees from Inovio Pharmaceuticals related to DNA vaccine development. DBW has received grant funding, participates in industry collaborations, has received speaking honoraria, and has received fees for consulting, including serving on scientific review committees and board series. Remuneration received by DBW includes direct payments, stock, or stock options, and, in the interest of disclosure, he notes potential conflicts associated with his work with Inovio Pharmaceuticals and possibly others. MCW and DBW have a pending US patent, 62750213.

Copyright: © 2020, American Society for Clinical Investigation.

Submitted: August 19, 2019; **Accepted:** October 24, 2019; **Published:** January 6, 2020.

Reference information: *J Clin Invest.* 2020;130(2):827–837.

<https://doi.org/10.1172/JCI132779>.

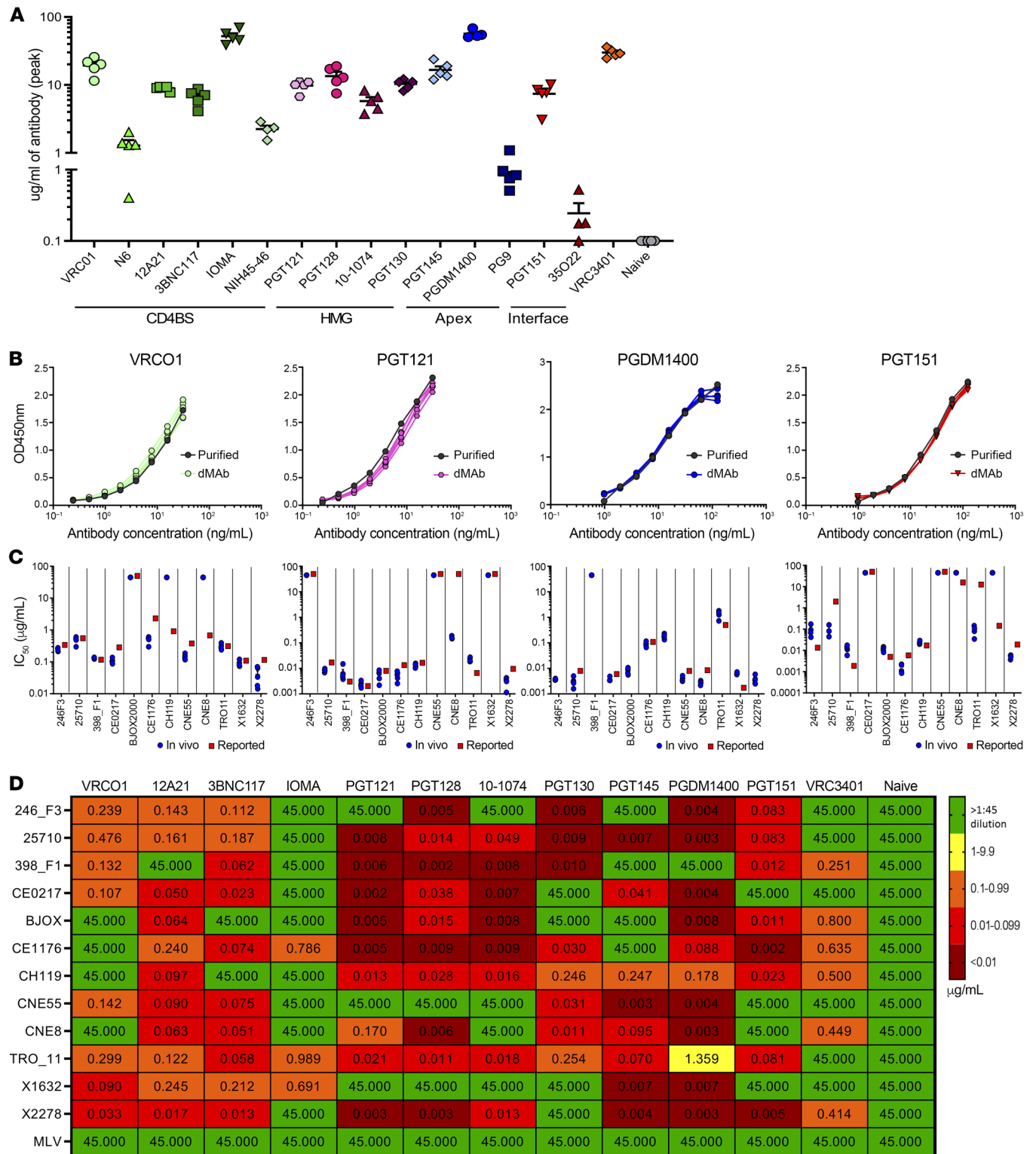


Figure 1. In vivo expression of dmAb-encoded HIV-1 bNAbs in mice. (A) Peak dmAb expression levels (d14) of bNAbs in the sera of transiently immunodepleted mice. Groups of mice ($n = 5$) were administered dmAb constructs expressing 1 of 16 different bNAbs. (B) Binding curves for 4 dmAbs against HIV-1 trimer BG505_MD39. Serum dmAb levels were normalized for expression (colored lines, $n = 5$ mice) and compared with the similar purified recombinant protein (black lines) over various concentrations. (C) Individual mouse IC₅₀ ($n = 5$) for 4 dmAbs across the 12 viruses of the global panels (blue circles) versus values reported in the literature (red squares). Literature values gathered from Los Alamos CATNAP. (D) Mean ($n = 5$) IC₅₀ pseudotype neutralization of d14 mouse sera against the 12 viruses of the global panel and MLV control. Value of 45 corresponds to no neutralization at a 1:45 dilution, the lowest dilution of the mouse serum tested. All other values are in μg/ml. Horizontal bars indicate mean; error bars represent SEM. Expression levels are representative of 2 experimental replicates; binding and neutralization testing were performed once.

induce protective levels of antibody in mice against important infectious disease targets, including influenza A and B viruses, *Pseudomonas aeruginosa*, Zaire Ebola virus, dengue virus, Zika virus, and chikungunya virus (16–21).

Here, we studied the activity of a panel of 16 engineered dmAbs encoding HIV-1-specific mAbs that exhibit broad neutralizing activity. Following dmAb administration, we observed rapid expression and sustained blood levels for months in small animals. These in vivo-produced dmAbs were functionally active and neutralized to varying degrees the 12 global panel viruses in an envelope-pseudotyped virus-neutralization assay (22). To decrease the possibility of viral escape, we next explored administration of multiple (up to 4) dmAbs into a single animal and demonstrated expansion of serum-neutralizing breadth. Based on in vivo dmAb levels and neutralizing potency, we advanced 2 dmAbs, PGT121 and PGDM1400, for a pilot NHP study. In this study, NHPs were delivered a single dmAb (PGDM1400) or a combination of the 2 (PGT121 and PGDM1400). Strong expression was observed in both groups, with a range from 6 to 34.3 $\mu\text{g}/\text{ml}$ at peak levels. All animals expressed dmAbs, and the serum demonstrated strong tier-2 neutralization breadth. Additionally, the levels of dmAb observed in this study were, on average, more than 10 times higher compared with an initial NHP dmAbs study (21). This provides evidence for further development of this platform, which represents an alternative modality for in vivo antibody production against HIV-1 and other biological targets.

Results

Robust expression of optimized HIV-1 dmAbs expressed in vitro and in vivo. dmAbs utilize optimizations that were developed to increase plasmid uptake and expression in context of delivery by adaptive electroporation (23). These improvements resulted in substantial enhancement of in vivo expression launched from plasmids. Here, we adapted multiple HIV-1-specific bNAbs and tested their expression and in vivo levels. We compared 16 different bNAbs targeting 5 different regions of the HIV-1 envelope: CD4-binding site (VRC01, N6, 12A21, 3BNC117, IOMA, NIH45-46); high-mannose glycan patch (PGT121, PGT128, 10-1074, PGT130); apex (PGT145, PGDM1400, PG9); gp120-gp41 interface (PGT151, 35O22); and gp41 fusion domain (VRC34.01) (2, 24–27). bNAbs encoded as dmAbs were selected based on target epitope, neutralization capacity, and other characteristics, such as length of heavy chain (HC) complementarity-determining regions 3 (CDR3) and percentage of somatic hypermutation, to obtain a range of antibody characteristics (Supplemental Table 1; supplemental material available online with this article; <https://doi.org/10.1172/JCI132779DS1>). The HC length of the CDR3 region ranged from 12 (3BNC117) to 35 (PGDM1400), with an average length across all dmAbs of 22. The percentage of amino acid somatic mutations from germline in the HC ranged from 18% (IOMA) to 42% (VRC01), with an average of 28%. Plasmids encoding the HC or the light chain (LC) of each of the bNAbs were RNA and codon optimized, synthesized, and cloned into the modified pVax1 backbone. All dmAbs were of the human IgG1 (hIgG1) isotype. Expression levels in vitro of all dmAbs were confirmed using transient transfection of HEK 293T cells (Supplemental Figure 1).

Next, we proceeded to assess in vivo expression in transiently immunodepleted mice to prevent the development of antidrug antibody (ADA) responses against the hIgG1. Mice were injected with plasmid dmAb constructs followed by intramuscular electroporation (IM-EP) using the CELLECTRA-3P device. We observed dmAb expression in sera 2 days after injection, with peak levels around d21 (Supplemental Figure 2). dmAb was continuously detected in the sera for over 300 days. Peak levels of dmAbs varied from below 1 $\mu\text{g}/\text{ml}$ to greater than 80 $\mu\text{g}/\text{ml}$ (Figure 1A). The majority of dmAbs exhibited peak levels between 10 and 30 $\mu\text{g}/\text{ml}$. There was minimal variability among mice receiving a given dmAb, supporting a model in which the intrinsic properties of each antibody sequence influence the overall levels observed in vivo. We did not observe any correlation in dmAb levels for different families, HC CDR3 length, or percentage of somatic hypermutation rate of the HC.

Functionality of in vivo-produced dmAbs is comparable to recombinant mAb counterparts. To further characterize in vivo-produced dmAbs, we investigated their ability to bind to trimer as compared with recombinantly produced mAbs. We observed similar strength of binding to trimer as compared with recombinant protein mAb for all tested dmAbs (Figure 1B and Supplemental Figure 3A). In agreement with our other dmAb studies, this suggests proper folding of the dmAbs in vivo and supports retention of their antigen specificity (16–20).

We next examined dmAb functionality in the context of neutralization using HIV-1 envelope pseudotyped viruses representing the global diversity of HIV-1 glycoprotein (22). We observed strong neutralization titers for all the studied dmAbs (Figure 1, C and D). Importantly, there was low variability in neutralization titers among mice given a specific dmAb based on each specific group and serum neutralization titers (IC_{50}) were similar to titers reported in the literature (Figure 1C and Supplemental Figure 3B). The neutralization data further confirm dmAbs were assembled, formed, and properly folded in vivo and then exhibited potency similar to that of the recombinant protein mAbs.

Modifications improved production of low-expressing N6 dmAb. N6 is an extremely potent and broad neutralizing anti-HIV-1 antibody (24); however, its in vivo levels were among the 3 lowest (Figure 1A). Based on these previous studies, we observed that single amino acid modification can significantly increase dmAb expression (16). Thus, we sought to increase its expression by designing modifications to both the HC and light chain (LC) of the original N6 amino acid sequence at the C- and N-terminus of the variable region. These modifications were selected to make the antibody more similar to the human parental germline antibody sequence (Supplemental Figure 4A). Mice injected with HC unmodified + LC modified (LC_{mod}) or HC modified + LC unmodified (HC_{mod}) dmAb had 3.5-fold increases in levels over the unmodified original N6 (Supplemental Figure 4B). When both modified plasmids were used to assemble modified N6 (N6_{mod}), levels increased 9-fold over unmodified and 2.5-fold over each modified chain. Modifications to the variable regions can change an antibody's ability to bind to its target and affect its functionality. Binding to trimer was similar between serum from mice injected with N6_{mod} dmAb and recombinant unmodified N6 (Supplemental Figure 4C). Furthermore, recombinant antibodies expressing either N6 or N6_{mod}

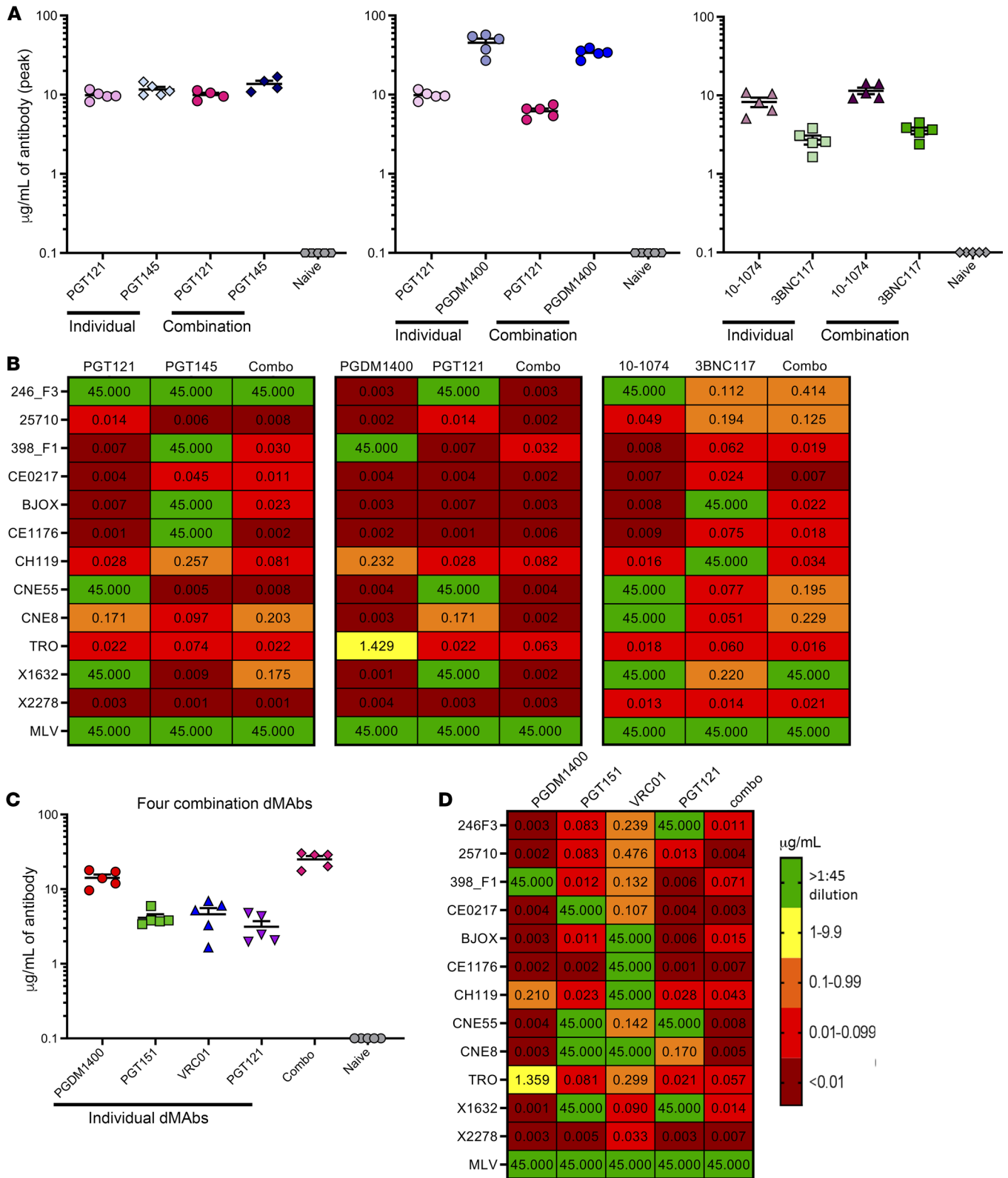


Figure 2. Delivery of multiple dmAb constructs in a single mouse maintains individual dmAb expression levels and increases serum neutralization breadth. (A) Groups of mice ($n = 5$) were administered a single dmAb (PGT121, PGT145, PGDM1400, 3BNC117, or 10-1074) or a combination of 2 dmAbs (PGT121+PGT145, PGDM1400+PGT121, 3BNC117+10-1074). Peak serum expression levels of human IgG were quantified by ELISA. (B) Mean ($n = 5$) IC_{50} pseudotype neutralization against the 12 viruses of the global panel and MLV control of sera collected at d14 from mice administered a single or 2 dmAbs. Value of 45 corresponds to no neutralization at a 1:45 dilution, the lowest dilution of the mouse serum tested. All other values are in $\mu\text{g}/\text{mL}$. (C) Total human IgG serum expression levels following administration of individual dmAbs (PGDM1400, PGT151, VRC01, and PGT121) and coadministration of all 4 dmAbs (combo) in mice ($n = 5$). (D) Mean ($n = 5$) IC_{50} pseudotype neutralization against the 12 viruses of the global panel and MLV for sera collected from mice administered individual dmAbs and combination of the 4 dmAbs. Horizontal bars indicate mean; error bars represent SEM. Expression levels are representative of 2 experimental replicates; binding and neutralization testing were performed once.

were able to neutralize multiple viruses from the global panel to degrees similar to those of levels previously reported in the literature (Supplemental Figure 4D and ref. 24). Thus, these modifications appear to be important for increasing overall production *in vivo*, resulting in increased serum levels of antibody while maintaining the functionality of this antibody. While there was marked improvement in the *in vivo* production levels of N6_{mod}, these levels remained on the lower end and additional rounds of optimization could further improve *in vivo* levels.

Delivery of multiple dmAbs to provide enhanced coverage of viral mutations. Due to the high error rate of HIV-1 reverse transcription and resultant high antigenic variability, viral immune escape from a single-antibody therapy is likely (7). Additionally, escape mutations to the mAb may already exist in populations, as no single mAb targets all circulating HIV-1 strains (7). In order to overcome such issues, we evaluated codelivery of multiple bNAbs against distinct HIV-1 envelope epitopes in the dmAb delivery platform. We selected 2 combinations that are currently in clinical trials, 3BNC117+10-1074 (5, 6) and PGDM1400+PGT121 (NCT03205917) as well as PGT121+PGT145. PGT121 and PGT145 were chosen based on *in vivo* dmAb levels, target epitope, and neutralization profiles of the antibodies. Mice were dosed with either a single dmAb construct or with 2 dmAb constructs in separate distinct muscle sites. *In vivo* levels of each individual antibody were similar in the combination mice as compared with mice delivered only a single antibody (Figure 2A). Individually, bNAb targets between 7 and 11 viruses in the global panel with various gaps in neutralization capacity (Figure 1C). By expressing 2 dmAbs in a single mouse, we observed an increase in their overall breadth of neutralization, targeting never less than 11 different members of the global panel as compared with each of the individual dmAbs with the PGDM1400+PGT121 (NCT0320591) combination now providing 100% viral coverage (Figure 2B and ref. 28).

We next sought to deliver and express 4 dmAbs in a single mouse using antibodies PGDM1400, PGT151, VRC01, and PGT121. Such deliveries of multiple antibodies are difficult using other methods. For this study, the antibodies were selected based on their neutralization capacity, overall *in vivo* levels, and ability to target distinct epitopes on the HIV-1 envelope. In these studies, animals were injected with a single dmAb or with all 4. As we do not have anti-idiotypic antibodies for these antibodies, we measured the total amount of the xenogeneic human antibody expressed in the mice (Figure 2C). The total serum hIgG1 dmAb levels in the mice administered with all 4 dmAb constructs were comparable to the sum of the levels of each dmAb construct administered individually (sum of mice injected with the individual dmAbs: 26.01 $\mu\text{g}/\text{ml}$ vs. combination dmAb mice: 25.10 $\mu\text{g}/\text{ml}$). Once again, we observed increased neutralization breadth in the sera of mice that received all 4 dmAb constructs compared with neutralization breadth in the sera of mice that received each individual dmAb construct (Figure 2D). By delivering all 4 dmAb constructs at once, we observed neutralization IC_{50} levels below 0.1 $\mu\text{g}/\text{ml}$ across the entire global panel.

HIV-1 dmAbs expression in NHPs. Based on the promising studies in mice, we next explored dmAb delivery of HIV-1-specific dmAbs in a pilot NHP animal model, which is more relevant for translation to humans. Two dmAbs were selected to move into NHPs, PGDM1400 and PGT121, based on high *in vivo* dmAb levels in mice (Figure 1). Two groups of 4 macaques were dosed with

either 6 mg of PGDM1400 dmAb plasmid construct (group 1) or 3 mg of PGDM1400 plus 3 mg of PGT121 dmAb plasmid construct (group 2). Expression of hIgG1 was detected in NHP serum as early as 3 days after injection and peaked at d14 (Figure 3A, Supplemental Figure 5A, and Supplemental Figure 6A). Total hIgG1 levels at peak were slightly higher for the group receiving PGDM1400 dmAb alone (group 1) compared with the 2 dmAbs PGDM1400 and PGT121 (group 2) (Figure 3B). The total hIgG1 detected in the serum from group 1 ranged between 11.2 and 34.3 $\mu\text{g}/\text{ml}$ (mean 25.1 $\mu\text{g}/\text{ml}$) and for group 2 between 6.3 and 20.4 $\mu\text{g}/\text{ml}$ (mean 10.1 $\mu\text{g}/\text{ml}$). The levels of hIgG1 dmAb in the sera declined after d14 to undetectable levels by d35, which is expected in this context in which a xenogeneic human IgG was being expressed in an immune-competent NHP host (29–31). Accordingly, the decrease in dmAb levels after d14 corresponded with the development of NHP anti-human IgG-dmAb antibodies in the sera (Supplemental Figure 5B and Supplemental Figure 6B). Using envelope antigen and secondary antibodies specifically recognizing hIgG1- κ (PGDM1400) versus hIgG1- λ (PGT121) LCs, we were able to confirm expression of both PGDM1400 and PGT121 dmAbs in group 2 NHP sera (Figure 3C, Supplemental Figure 5C, and Supplemental Figure 6C).

We proceeded to determine the antiviral activity of the sera harboring the anti-HIV-1 dmAbs. Prebleed sera (d0) and sera from the peak dmAb level time point (d14) were tested for neutralization against the global panel tier-2 viruses. NHP sera contained no neutralizing antibodies before dmAb administration (d0), and no nonspecific neutralization was detected against mouse leukemia virus (MLV) on d0 and d14 (Table 1). Sera collected at peak dmAb levels were able to neutralize 11 out of 12 viruses (group 1) and 12 out of 12 viruses (group 2) (Figure 3D and Table 1). For several viruses, specifically 243F6, 25710, CE0217, CNE55, and CNE8, titers (IC_{50}) for both groups were less than 0.1 $\mu\text{g}/\text{ml}$. These pseudotype neutralization titers, originally performed at The Wistar Institute, were then retested and confirmed at Duke University. Similar group 1 and group 2 NHP neutralization titers (IC_{50}) were obtained across the 9 HIV-1 pseudotype viruses reevaluated (Supplemental Figure 7A). Delivery of a second dmAb in group 2 modestly improved neutralization for some isolates and added neutralization coverage for 2 additional viruses, 398F1 and TRO.11. We further explored the antiviral activity by exploring the antibody-dependent cell-mediated cytotoxicity (ADCC) against a subtype C HIV-1 infectious molecular clone (IMC) DU151-infected cells, chosen based on sensitivity to both mAbs. Though ADCC activity of the serum was usually only detected at concentrations of more than 4 $\mu\text{g}/\text{mL}$, it was comparable to the recombinant protein mAb activity (Figure 3E). No ADCC activity was observed for the negative control recombinant palivizumab antibody (Supplemental Figure 7B). In summary, the NHP data support that HIV-1 dmAbs expressed at high levels bind to envelope trimers, neutralize numerous tier-2 viruses, have effector functions, and can complement each other *in vivo*.

Discussion

Recently, the use of protein mAbs has become a first-line treatment for numerous cancers and similarly plays a major role in autoimmune disease therapies (32). In general, the adoption of mAbs for infectious disease is very exciting, but to date, there have been lim-

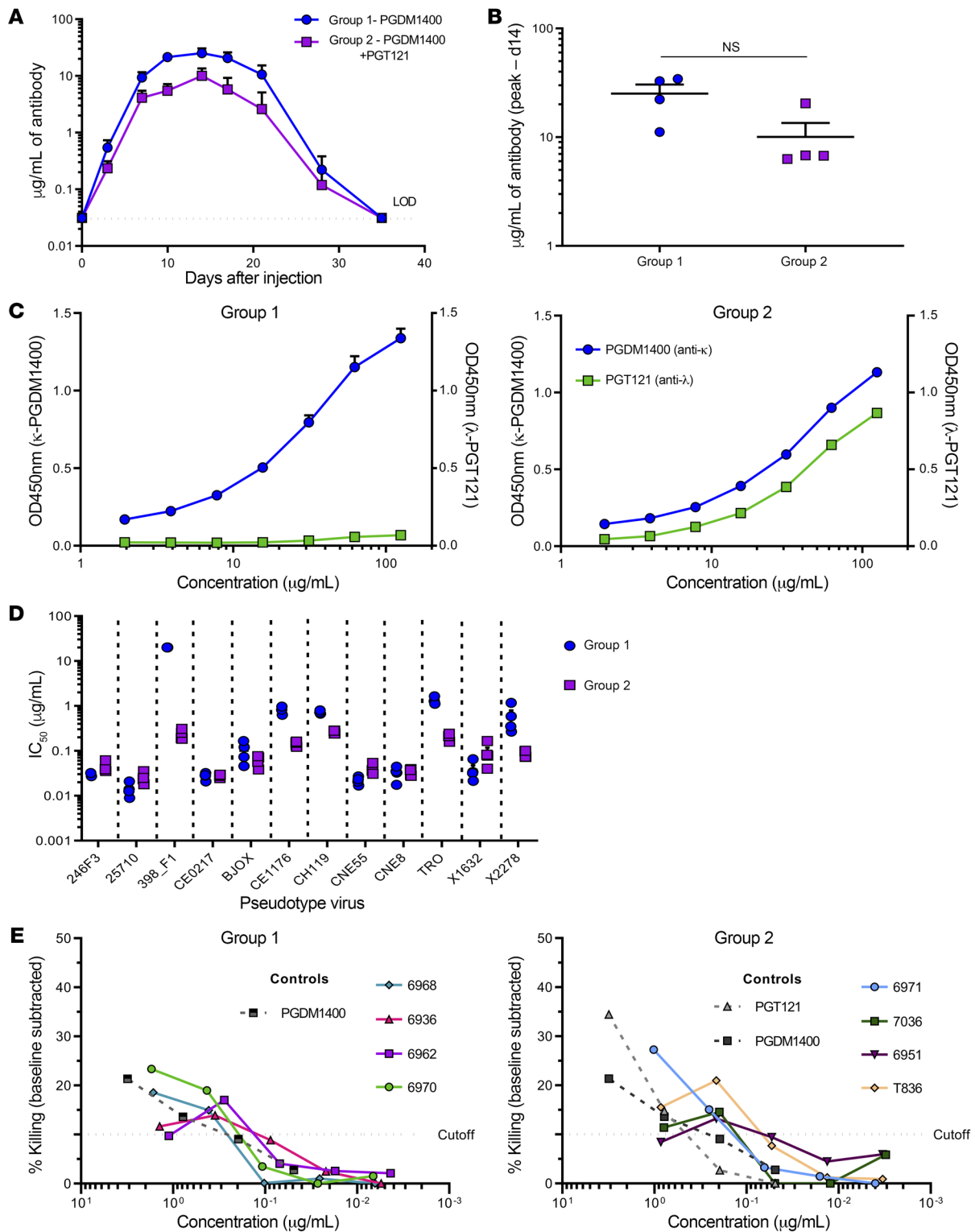


Figure 3. PGDM1400 and PGT121 are expressed as dmAbs in NHPs. Immune-competent macaques were injected with hlgG1 dmAb constructs (d0) and serially bled. Group 1 animals ($n = 4$) received 6 mg of PGDM1400-encoding plasmid DNA; group 2 animals ($n = 4$) received 3 mg of PGDM1400 and 3 mg of PGT121 plasmid DNA. (A) Quantification of hlgG1 in the sera of group 1 and group 2 NHPs over time. (B) Peak expression levels of total hlgG1 for each group at d14. (C) Serum-binding curves against HIV-1 Env trimer, BG505_MD39, using different secondary antibodies to establish the binding of PGDM1400 (hlgG1- κ LC, blue) and PGT121 (hlgG1- λ LC, green). (D) Neutralization IC₅₀ of serum across the 12-virus global pseudotype panel using serum from peak dmAb expression (d14). (E) Baseline subtracted ADCC-killing activity of serum for IMC DU151 compared with recombinant mAbs PGDM1400 and PGT121. Horizontal bars indicate mean; error bars represent SEM. Expression levels and neutralization titers are representative of 2 replications; all other tests were performed once. Two-tailed Student's t test was performed to determine significant differences in levels of expression between group 1 and group 2. $P < 0.05$ was considered significant.

Table 1. Neutralization ID₅₀ of dmAb-treated NHP serum across the global panel

| | 246F3 | | 25710 | | 398F1 | | CE0217 | | BJOX | | CE1176 | | CH119 | | CNE55 | | CNE8 | | TRO.11 | | X1632 | | X2278 | | MLV | | |
|---------|---------|-----|-------|-----|--------|-----|--------|-----|-------|-----|--------|-----|-------|-----|-------|-----|--------|-----|--------|-----|-------|-----|-------|-----|-------|-----|-----|
| | NHP ID | d0 | d14 | d0 | d14 | d0 | d14 | d0 | d14 | d0 | d14 | d0 | d14 | d0 | d14 | d0 | d14 | d0 | d14 | d0 | d14 | d0 | d14 | d0 | d14 | d0 | d14 |
| Group 1 | 6970 | <20 | 1262 | <20 | 3834 | <20 | <20 | <20 | 1646 | <20 | 752 | <20 | 54 | <20 | 51 | <20 | 2041 | <20 | 1049 | <20 | 27 | <20 | 1022 | <20 | 128 | <20 | <20 |
| | 6962 | <20 | 808 | <20 | 1597 | <20 | <20 | <20 | 795 | <20 | 185 | <20 | 27 | <20 | 31 | <20 | 826 | <20 | 638 | <20 | 20 | <20 | 690 | <20 | 38 | <20 | <20 |
| | 6963 | <20 | 349 | <20 | 880 | <20 | <20 | <20 | 348 | <20 | 153 | <20 | <20 | <20 | <20 | <20 | 539 | <20 | 251 | <20 | <20 | <20 | 521 | <20 | 32 | <20 | <20 |
| | 6968 | <20 | 994 | <20 | 1571 | <20 | <20 | <20 | 1149 | <20 | 199 | <20 | 34 | <20 | 41 | <20 | 1403 | <20 | 1877 | <20 | 20 | <20 | 501 | <20 | 28 | <20 | <20 |
| | Average | <20 | 853.3 | <20 | 1970.5 | <20 | <20 | <20 | 984.5 | <20 | 322.3 | <20 | 28.8 | <20 | 30.8 | <20 | 1202.3 | <20 | 953.8 | <20 | 20.0 | <20 | 683.5 | <20 | 56.5 | <20 | <20 |
| Group 2 | 6971 | <20 | 333 | <20 | 581 | <20 | 107 | <20 | 824 | <20 | 286 | <20 | 154 | <20 | 84 | <20 | 568 | <20 | 520 | <20 | 128 | <20 | 123 | <20 | 209 | <20 | <20 |
| | 7036 | <20 | 176 | <20 | 268 | <20 | 34 | <20 | 255 | <20 | 164 | <20 | 51 | <20 | 26 | <20 | 167 | <20 | 216 | <20 | 38 | <20 | 157 | <20 | 86 | <20 | <20 |
| | 6951 | <20 | 175 | <20 | 379 | <20 | 27 | <20 | 245 | <20 | 119 | <20 | 45 | <20 | 24 | <20 | 127 | <20 | 244 | <20 | 32 | <20 | 87 | <20 | 92 | <20 | <20 |
| | T863 | <20 | 186 | <20 | 270 | <20 | 22 | <20 | 230 | <20 | 89 | <20 | 42 | <20 | 24 | <20 | 218 | <20 | 181 | <20 | 28 | <20 | 82 | <20 | 67 | <20 | <20 |
| | Average | <20 | 217.5 | <20 | 374.5 | <20 | 60.5 | <20 | 388.5 | <20 | 164.5 | <20 | 73.0 | <20 | 37.0 | <20 | 270.0 | <20 | 290.3 | <20 | 56.5 | <20 | 112.3 | <20 | 113.5 | <20 | <20 |

ID₅₀ neutralization titers for heat-inactivated serum from d0 and d14 for NHP administered dmAb PGDM1400 (group 1) or PGDM1400 and PGT121 (group 2) across the global panel of pseudotype HIV-1 envelopes and nonspecific MLV control. Red indicates titers higher than 1000; orange indicates titers between 500–1000; purple indicates 100–500; blue indicates 45–100; and green indicates below 45.

ited approvals (32). Due to the exceptional breadth and potency of mAbs, clinical trials are in progress to explore the ability of bNAb against HIV-1 to both prevent and treat infection (7). Additional strategies for delivery are likely important, especially for providing these strategies in the developing world (33). In this manuscript, we describe a recently developed dmAb platform for delivering bNAb and provide what we believe is the first proof of concept for this delivery targeting HIV-1.

Through iterative studies, we describe dmAb delivery resulting in expression of multiple HIV-1-specific antibodies up to 80 µg/ml in mice. To date, in vitro expression of bNAb from transfected cell lines does not correlate or predict in vivo levels when delivered via the dmAb platform (16). Interestingly, similar variations in dmAb levels across multiple different antibodies were observed with AAV-mediated gene delivery (12, 29, 34). Even within the same class of antibodies that share the germline VH gene (IGHV1-2) usage, dmAb levels vary significantly, between 1.3 µg/ml (N6) and 52.2 µg/ml (IOMA) (Figure 1A). Furthermore, we did not observe any correlation of in vivo levels and HC CDR3 length, LC usage, or rate of somatic hypermutation. We demonstrate that modifications to the beginning and end of N6 variable regions of the HCs and LCs improved in vivo levels while maintaining the antibody’s activity (Supplemental Figure 4). As we acquire more data on antibody sequences and dmAb expression, a better understanding of in vivo sequence liabilities will be obtained. As HIV-1 bNAb are highly somatically mutated and many of these mutations are required for maintaining the functionality of the antibody, balancing mutations made for increasing dmAb levels will need to be weighted with impacts on functionality. dmAbs are an important tool for these studies, since DNA can be easily modified to encode different amino acids and the effects on both in vivo expression and functionality can be quickly and cost-effectively explored. Furthermore, the mAb sequence rules that dictate the in vivo expression of dmAbs delivered to muscle tissue could translate to other platforms, such as AAV, where muscle expression is also being tested.

We demonstrated the ability to encode 2 HIV-1-specific bNAb in NHPs using the dmAb technology. We observed dmAb expression in NHP sera within 3 days of dmAb administration and levels that peaked around d14. We believe these peak levels (ranging from 6 to 34 µg/ml) would be protective against multiple SHIV strains upon challenge based upon prior studies that utilized recombinant mAb protein (4, 28, 35–37). Specifically, Julg et al. demonstrated that NHPs received passive infusions of PGDM1400 one day prior to SHIV-325c challenge at 2 mg/kg and 0.4 mg/kg doses were protected from infection (28). The average levels of PGDM1400 in the serum at time of challenge were 6.9 and 2.5 µg/ml for 2 and 0.4 mg/kg infusions, respectively. There was breakthrough infection in the group delivered 0.08 mg/kg, which corresponded to a serum level of 0.22 µg/ml at the time of challenge. Additionally, PGT121 demonstrated protection against SHIV-SF162P3 and SHIV-AD8EO at levels of 15 and 22 µg/ml, respectively, with partial infection at serum levels of 1.8 µg/ml (36, 37). In the context of treatment, NHPs chronically infected with SHIV-SF162P3 and delivered a single infusion of 10 mg/kg of PGT121 were able to control viral loads to undetectable levels (38). Rebound occurred in 3 out of 4 animals once mAb serum concentrations reached undetectable levels (<1 µg/ml), with 1 animal having long-term virologic control. While we are unaware of a prior study for the use of PGDM1400 in a preclinical treatment setting, the peak levels of this antibody in the NHPs might be relevant in therapeutic settings, especially considering that the mean concentrations of 3BNC117 and 10-1074 were between 1.9 and 14.8 µg/ml at the time of viral rebound in the study by Mendoza et al. (6). However, additional testing of the ability of dmAbs that are developed as species-matched antibodies to affect challenge outcomes or control infection will be informative.

There was a decline in human dmAb levels the NHP study observed after d14 that corresponded with the development of ADA due to the expression of the xenogeneic protein. The development of ADA against a cross-species human IgG has also been

observed in NHPs following AAV, recombinant protein (30), RNA (39), and adenovirus delivery of antibodies in mice (40). In studies of AAV delivery of HIV-1/SIV bNAbs, induction of ADA was closely associated with the distance of the variable regions from germline (31). Furthermore, AAV delivery of anti-SIV mAbs that were originally isolated from Rhesus Macaques led to a lower incidence of ADA responses in the recipient NHPs (34). In mice, we eliminated host immune responses to hIgG1 dmAb via transient immunosuppression. Additionally, we have observed that using a species-matched fully murine dmAb in mice can avoid significant ADA development and allow for systemic expression of dmAbs in recipient mice for several months (41). However, we have not yet developed fully simian dmAbs, and future studies will test this principle. Ultimately, human studies will be particularly informative. In this regard, recent mAb delivery clinical trials include an AAV vector encoding HIV-1 bNAb VRC07 (NCT03374202), what we believe is the first dmAb construct for expression of antibody against Zika virus (NCT03831503), and an mRNA platform for delivery of anti-chikungunya virus antibody (NCT03829384); these will be particularly valuable for providing additional information on this important question.

Depending on the application of the mAb, different effector functions and modifications in the antibody Fc domain may be required. mAbs used for HIV-1 prevention and treatment will likely benefit from longer *in vivo* half-lives. Amino acid mutations to the Fc, including YTE and LS, yield prolonged recombinant *in vivo* antibody half-lives in both preclinical NHP studies and in the clinic (42). We have previously demonstrated the feasibility of dmAbs for encoding Fc modifications such as the LALA mutation to prevent antibody-dependent enhancement (ADE) in dengue virus infection (20). Furthermore, modifications to the Fc region of the antibody can increase ADCC activity, which is important in HIV-1 protection and control of infection (43). Inclusion of these modifications to increase activity of dmAb against infected cells is imperative for therapeutic cure approaches. Exploration of half-life extension and Fc activity modification for HIV-1 dmAbs is ongoing.

Our data describe what we believe is a new important technology for *in vivo* HIV-1 antibody delivery. We demonstrate that dmAb constructs can be developed to encode multiple HIV-1-specific IgG1 and that the *in vivo*-expressed dmAbs retain their functional activity in both small and large animals. The observation that *in vivo*-produced dmAbs had HIV-1 envelope trimer binding and neutralization capacity similar to that of their recombinantly produced counterparts highlights the effective folding of the dmAb antibody in this system. Furthermore, the ability to deliver multiple antibodies, in this case four at one time, to limit viral escape and resistance may be important for HIV-1 prevention and treatment strategies. To our knowledge, this is the most comprehensive screening of multiple HIV-1 antibodies delivered by the same platform, demonstrating how inherent antibody characteristics influence *in vivo* production. Additionally, through numerous optimization efforts aiming at both DNA synthetic design and delivery technology, we were able to consistently reach greater than 5 $\mu\text{g}/\text{ml}$ antibody in NHPs, with some NHPs reaching serum levels of more than 30 $\mu\text{g}/\text{ml}$. These levels represent a substantial improvement compared with the original NHP dmAb studies, which achieved on average a tenth the *in vivo* production observed here (21). These studies demonstrate the possibility of dmAbs as an approach to delivery of mAb specificities in a simple to produce, temperature-stable, and rapid-delivery format. Further study of the dmAb platform for anti-HIV strategies appears to be important.

Methods

DNA design and plasmid synthesis

Protein sequences for HIV-1 antibodies were obtained from NCBI GenBank (Supplemental Table 1). The DNA sequences were RNA and codon optimized, as previously described (16–18, 20). Leader sequences were added to the beginning of the HC and LC of the antibody. The HC and LC were synthesized and cloned (Genscript) into a modified mammalian pVAX1 expression plasmid (Thermo Fisher). Plasmids encoding the 12–global panel HIV envelope gp160 for the TZM-bl neutralization assay and a plasmid encoding the murine leukemia virus (MLV) envelope as an antibody-nonspecific pseudotype control were obtained from the NIH AIDS Reagent Program (Division of AIDS, National Institute of Allergy and Infectious Diseases [NIAID], NIH).

Cell lines, transfection, and recombinant antibody purifications

HEK 293T cells (ATCC) and TZM-bl cells (NIH AIDS Reagent Program) were maintained in DMEM (Thermo Fisher) supplemented with 10% heat-inactivated FBS (Atlas Biologicals). Expi293F cells (Thermo Fisher) were maintained in Expi293 expression medium (Thermo Fisher). All cell lines were mycoplasma negative. HEK 293T cells were transfected with HIV-1 bNAb-encoding dmAb plasmids using GeneJammer (Agilent) transfection reagent following the manufacturer's protocol. Two days after transfection, media and cells were harvested and lysed with cell lysis buffer (Cell Signaling Technology) modified with cOmplete EDTA-free protease inhibitor cocktail (Roche). To produce recombinant HIV mAbs for assay and controls, Expi293F cells were transfected following the manufacturer's protocol for Expifectamine (Thermo Fisher). Transfection enhancers were added 18 hours after transfection, and supernatants were harvested 6 days after transfection. Protein G agarose (Thermo Fisher) was then used following the manufacturer's protocol to purify the IgG. Recombinant antibody purity was confirmed with Coomassie staining of SDS-PAGE gels and quantified using the quantification ELISA described below.

Trimer production

Expi293F cells were transfected with plasmid expressing the HIV-1 gp160 Env trimer BG505_MD39_His construct. Cell supernatants containing trimer were clarified by centrifuging (4000 g, 25 minutes) and filtering (0.2 μm Nalgene Rapid-Flow Filter). Trimers were then purified from supernatants by nickel affinity chromatography on a HIS-TRAP HP column (GE Healthcare). The trimers were then purified over a size-exclusion chromatography column (GE S200 Increase) in PBS. The molecular weight and homogeneity of the trimers were confirmed by protein-conjugated analysis from ASTRA software (Wyatt Technology) with data collected from a size-exclusion chromatography multi-angle light scattering (SEC-MALS) experiment run in PBS using a GE S6 increase column, followed by DAWN HELEOS II and Optilab T-rEX detectors. The trimers were aliquoted at 1 mg/ml and flash-frozen in thin-walled PCR tubes prior to use.

ELISA

dmAb quantification ELISA for mouse. DNA-encoded mAb levels were quantified as previously described (16). Briefly, high-binding polystyrene 96-well plates (Thermo Fisher) were coated with unconjugated purified goat anti-human IgG-Fc (1 µg/ml) overnight in PBS. After blocking with 10% newborn calf serum (NCS), plates were washed with PBS containing 0.05% Tween-20. Mouse serum and standards were serially diluted and incubated for 1 hour at room temperature. Purified human IgG-κ (catalog P80-111, Bethyl Laboratories) and human IgG-λ (catalog P80-116, Bethyl Laboratories) were used as standards. After washing, plates were incubated with 1:20,000 dilution of either goat anti-human κ (catalog A80-115P, Bethyl Laboratories) or goat anti-human λ (catalog A80-116P, Bethyl Laboratories) LC secondary antibodies conjugated to HRP for 1 hour at room temperature. For quantification of total antibody levels in the mice dosed with 4 dmAb constructs, a secondary goat anti-human IgG H+L conjugated to HRP (catalog A80-119P, Bethyl Laboratories) was used. After washing, plates were developed with o-phenylenediamine dihydrochloride (OPD) substrate (SIGMAFAST OPD, Sigma-Aldrich). Plates were stopped with 2N H₂SO₄. Plates were read on a BioTek Synergy 2 plate reader (BioTek) at 450 nm and 570 nm wavelengths. Quantification of serum dmAb levels was determined by interpolating the unknown OD values to the standard curve.

dmAb quantification ELISA for NHP. Quantification for human IgG dmAb in NHP sera was determined using the Human Therapeutic IgG1 ELISA Kit (Cayman Chemicals) following the manufacturer's protocol. Serum was serially diluted to obtain 2 OD values within the linear range of the standard curve. Quantification measurements were repeated twice for d7 to d21.

dmAb binding to trimer ELISA. Binding curves of HIV serum-expressed dmAbs compared with recombinant proteins were obtained by coating 96-well half-area high-binding polystyrene plates (Thermo Fisher) with 1 µg/ml of rabbit anti-His antibody (catalog 25B6E11, Genscript) in PBS at 4°C. Plates were blocked with 5% skim milk in PBS with 1% NCS (Atlas Biologicals) and 0.2% Tween-20 for 1 hour at room temperature. His-BG505 MD39 trimer protein was then added at 1 µg/ml in PBS with 1% NBS and 0.2% Tween-20 for 2 hours at room temperature. Serum was normalized based on the quantification concentration and serially diluted 2-fold. A similar amount of purified recombinant mAb was added to match the serum concentration. Plates were incubated for 1 hour at 37°C. After washing, a 1:20,000 dilution of secondary goat anti-human κ (catalog A80-115P, Bethyl Laboratories) or goat anti-human λ (catalog A80-116P, Bethyl Laboratories) LC secondary antibodies conjugated to HRP was added and incubated for 1 hour at room temperature. Plates were then developed with 1-step ultra-3,3',5,5'-tetramethylbenzidine (TMB) substrate (Thermo Fisher) and read on a BioTek Synergy 2 plate reader (BioTek) at 450 nm and 570 nm wavelengths.

Anti-antibody detection ELISA. To determine the development of ADA development, 96-well half-area high-binding polystyrene plates (Thermo Fisher) were coated with 1 µg/ml of purified PGT121 or PGDM1400 (produced in-house) overnight in PBS at 4°C. Plates were then blocked with 5% skim milk in PBS with 1% NCS (Atlas Biologicals) and 0.2% Tween for 1 hour at room temperature. NHP serum was diluted 1:100, added to plates for each time point, and incubated for 1 hour at 37°C. After washing, a 1:20,000 dilution of secondary goat anti-NHP H+L min human secondary antibody conjugated to

HRP (catalog A140-202P, Bethyl Laboratories) was then added and incubated for 1 hour at room temperature. Plates were then developed with 1-step ultra-TMB substrate (Thermo Fisher) and read on BioTek Synergy 2 plate reader (BioTek) at 450 nm and 570 nm wavelengths.

Western blot

Western blots of transfected cell media were performed using 4%–12% Bis-Tris gels run with 2-(N-morpholino) ethanesulfonic acid (MES) buffer (Thermo Fisher). The gel was then transferred to a PVDF membrane (Millipore) and blocked with blocking buffer (LI-COR Bioscience) for 1 hour at room temperature. Membranes were then probed with IRDye-680RD anti-human secondary antibody (catalog 925-68078, LI-COR Bioscience) for 1 hour at room temperature. After washing, the membrane was scanned using the Odyssey CLx (LI-COR Bioscience). See complete unedited blots in the supplemental material.

Animals

Mice. Groups of five 6- to 8-week-old female BALB/c mice (Charles River) were transiently depleted of T cells as previously described (16) at the same time as receiving dmAb injection to attenuate mouse anti-human IgG anti-antibody immune responses. For experiments where a single dmAb was delivered, mice were injected with 100 µg (25 µg of HC and 25 µg of LC per site, 2 sites total) dmAb plasmids formulated with hyaluronidase (200 U/L, Sigma-Aldrich) and injected into the tibialis anterior muscles followed by IM-EP using the CELLECTRA-3P device (Inovio Pharmaceuticals). For experiments with 2 dmAb delivery, mice were injected with 100 µg (25 µg of HC and 25 µg of LC per site, 2 sites total) of each dmAb plasmid formulated with hyaluronidase into the tibialis anterior and quadriceps muscles followed by IM-EP. For experiments with 4 dmAb delivery, single dmAb control mice were injected with 50 µg (25 µg of HC and 25 µg of LC per site, 1 site total), which was formulated and injected into the tibialis anterior. Mice were injected with 50 µg DNA plasmid (25 µg of HC and 25 µg of LC per site, 1 site total), which was formulated and injected into the tibialis anterior and quadriceps muscles followed by IM-EP. Mice were serially bled to obtain serum for analysis.

NHPs. Two groups of cynomolgus macaques ($n = 4$) (Primigen) were treated with plasmid dmAb constructs encoding either PGDM1400 or PGDM1400 and PGT121, with animals receiving a total of 6 mg plasmid DNA. DNA was coformulated with hyaluronidase (Hylenex, 135 U/ml). Multi-depth IM injection was performed followed by electroporation using the Elgen1000 Twinjector (Inovio Pharmaceuticals). Macaques were serially bled to obtain serum over 60 days.

Ex vivo neutralization assay

Production of HIV envelope pseudotyped viruses and TZM-bl neutralization assay were performed as previously described (44). Pseudotyped viruses were produced using HEK 293T cells transfected with 4 µg of HIV Env plasmid and 8 µg of plasmid encoding the HIV backbone lacking Env (pSG3ΔEnv, NIH AIDS Reagent Program) using GeneJammer (Agilent). Forty-eight hours after transfection, media was collected, filtered, aliquoted, and stored at -80°C. Virus titers were determined to yield 150,000 relative light units (RLU) after 48 hours of infection. Mouse serum was heat inactivated for 15 minutes at 56°C, and NHP serum was inactivated for 30 minutes. Serum concentration was determined for 50% virus inhibition dilution (ID₅₀) and calculated using total human IgG quantification levels to determine the IC₅₀.

IMCs

HIV-1 reporter viruses used were replication-competent IMC designed to encode the *env* genes of DU151 (subtype C; GenBank DQ411851) in *cis* within a Nef-deficient isogenic backbone expressing the *Renilla* luciferase (Luc) reporter gene. All the IMCs were built using the original NL-LucR.T2A-ENV.ecto backbone as previously described (45). Reporter virus stocks were generated by transfection of 293T cells with proviral IMC plasmid DNA, and virus titers were determined on TZM-bl cells for quality control.

Infection of CEM.NKR_{CCR5} cell line with HIV-1 IMCs

CEM.NKR_{CCR5} (NIH AIDS Reagent Program) cells were infected with HIV-1 IMCs as previously described (46). Briefly, IMCs were titrated in order to achieve maximum expression within 48 to 72 hours after infection as determined by detection of Luc activity and intracellular p24 expression. IMC infections were performed by incubation of the optimal dilution of virus with CEM.NKR_{CCR5} cells for 0.5 hour at 37°C and 5% CO₂ in the presence of DEAE-dextran (7.5 µg/ml). The cells were subsequently resuspended at 0.5 × 10⁶/ml and cultured for 48 to 72 hours in complete medium containing 7.5 µg/ml DEAE-dextran. For each ADCC assay, the frequency of infected target cells was monitored by intracellular p24 staining. Assays performed using infected target cells were considered reliable if cell viability was 60% or more and the percentages of viable p24⁺ target cells on assay day were 20% or more.

Luc ADCC assay

ADCC activity was determined by a Luc-based assay as previously described (47). Briefly, CEM.NKR_{CCR5} cells were used as targets after infection with the HIV-1 IMCs. PBMCs obtained from an HIV-seronegative donor with the heterozygous 158F/V and 131H/R genotypes for FcγR3A and FcγR2A, respectively, were used as a source of effector cells and were used at an effector/target ratio of 30:1. Sera from NHPs inoculated with dmAb plasmids for PDGM1400 and PGT121 were initially diluted to reach an initial concentration ranging from 4 to 6 µg/ml of dmAb and tested across a range of concentrations using 5-fold serial dilutions. The reference mAbs were tested across a range of concentrations using 5-fold serial dilutions starting at 50 µg/ml. The effector cells, target cells, and Ab dilutions were plated in opaque 96-well half-area plates and were incubated for 6 hours at 37°C in 5% CO₂. The final read-out was the luminescence intensity (RLU) generated by the presence of residual intact target cells that had not been lysed by the effector population in the presence of ADCC-mediating mAb (ViviRen substrate, Promega). The percentage of specific killing was calculated using the following formula: percentage specific killing = [(number of RLU of target and effector well – number of RLU of test well)/number of RLU of target and effector well] × 100. In this analysis, the RLU of the target plus effector wells represents spontaneous lysis in the absence of any source of Ab. The ADCC detectable in NHP serum is reported after subtracting the activity observed in the serum before dmAb injection (baseline subtracted activity). Results were considered positive if the percentage of specific killing was greater than 15%. The RSV-specific

mAb palivizumab was used as a negative control, and a combination of C1/C2 A32, CD4bs CH44, glycosylation site 2G12, and gp41 7B2 mAbs (mAb mix) was used as a positive control.

Statistics

All statistics and calculations were performed using GraphPad Prism 7.0. dmAb levels in the serum were determined using the standard curve nonlinear regression model and interpolating values. ID₅₀ values were computed with a nonlinear regression model of percentage neutralization versus log reciprocal serum dilution. IC₅₀ values were determined using total human IgG quantification in the serum and the ID₅₀ titers. Linear regression analysis correlating various antibody characteristics with expression levels in vivo was also performed using GraphPad Prism. Two-tailed Student's *t* test or modified ANOVA was used to determine statistical significance. A *P* value of less than 0.05 was considered significant.

Study approval

All mouse experiments were carried out in accordance with animal protocol 112776 approved by the Wistar Institute IACUC. For the NHP expression study, cynomolgus macaques were housed at BIOQUAL according to the standards of the American Association for Accreditation of Laboratory Animal Care, and all animal protocols were IACUC approved.

Author contributions

MCW, ZX, DWK, LMH, and DBW were involved in study concept and design. MCW, ZX, ETR, CB, AT, AP, STCE, SK, MGK, JJ, PDF, SJR, TRFS, JM, DCM, and GF were involved in the acquisition, analysis, and interpretation of data. NC, KM, KEB, and DWK contributed crucial reagents. MCW, ZX, and DBW wrote the paper. All authors were involved in critically revising the manuscript. Authorship order for co-first authors was determined based on alphabetical order.

Acknowledgments

We would like to thank the Animal Facility staff at the Wistar Institute for providing housing and care to the animals. The following reagents were obtained through the NIH AIDS Reagent Program: Panel of Global HIV-1 Env Clones from David Montefiori, SV-AMLV-env from Nathaniel Landau and Dan Littman, HIV-1 SG3 ΔEnv noninfectious molecular clone and TZM-bl from John C. Kappes and Xiaoyun Wu, and CEM.NKR_{CCR5} cells from Alexandra Trkola. This work was supported by NIH IPCAVD grant U19 AI109646-04, WW Smith Charitable Trust grant 6743101374, and Martin Delaney Collaboration HIV Cure Research grant 2528109374 (to DBW).

Address correspondence to: David Weiner, Vaccine and Immunotherapy Center, Wistar Institute, 3601 Spruce Street Room 630, Philadelphia Pennsylvania, 19104, USA. Phone: 215.898.0381; Email: dweiner@wistar.org.

- Maartens G, Celum C, Lewin SR. HIV infection: epidemiology, pathogenesis, treatment, and prevention. *Lancet*. 2014;384(9939):258–271.
- McCoy LE, Burton DR. Identification and specificity of broadly neutralizing antibodies against

- HIV. *Immunol Rev*. 2017;275(1):11–20.
- Pegu A, Hessel AJ, Mascola JR, Haigwood NL. Use of broadly neutralizing antibodies for HIV-1 prevention. *Immunol Rev*. 2017;275(1):296–312.
- Gautam R, et al. A single injection of crystalliz-

- able fragment domain-modified antibodies elicits durable protection from SHIV infection. *Nat Med*. 2018;24(5):610–616.
- Bar-On Y, et al. Safety and antiviral activity of combination HIV-1 broadly neutralizing

- antibodies in viremic individuals. *Nat Med*. 2018;24(11):1701-1707.
6. Mendoza P, et al. Combination therapy with anti-HIV-1 antibodies maintains viral suppression. *Nature*. 2018;561(7724):479-484.
 7. Cohen YZ, Caskey M. Broadly neutralizing antibodies for treatment and prevention of HIV-1 infection. *Curr Opin HIV AIDS*. 2018;13(4):366-373.
 8. Bar KJ, et al. Effect of HIV antibody VRC01 on viral rebound after treatment interruption. *N Engl J Med*. 2016;375(21):2037-2050.
 9. Scheid JF, et al. HIV-1 antibody 3BNC117 suppresses viral rebound in humans during treatment interruption. *Nature*. 2016;535(7613):556-560.
 10. Awi NJ, Teow SY. Antibody-mediated therapy against HIV/AIDS: Where are we standing now? *J Pathog*. 2018;2018:8724549.
 11. Johnson PR, et al. Vector-mediated gene transfer engenders long-lived neutralizing activity and protection against SIV infection in monkeys. *Nat Med*. 2009;15(8):901-906.
 12. Balazs AB, Chen J, Hong CM, Rao DS, Yang L, Baltimore D. Antibody-based protection against HIV infection by vectored immunoprophylaxis. *Nature*. 2011;481(7379):81-84.
 13. Saunders KO, et al. Broadly neutralizing human immunodeficiency virus type 1 antibody gene transfer protects nonhuman primates from mucosal simian-human immunodeficiency virus infection. *J Virol*. 2015;89(16):8334-8345.
 14. Fuchs SP, Desrosiers RC. Promise and problems associated with the use of recombinant AAV for the delivery of anti-HIV antibodies. *Mol Ther Methods Clin Dev*. 2016;3:16068.
 15. Priddy FH, et al. Adeno-associated virus vectored immunoprophylaxis to prevent HIV in healthy adults: a phase 1 randomised controlled trial. *Lancet HIV*. 2019;6(4):e230-e239.
 16. Patel A, et al. In vivo delivery of synthetic human DNA-encoded monoclonal antibodies protect against ebolavirus infection in a mouse model. *Cell Rep*. 2018;25(7):1982-1993.e4.
 17. Patel A, et al. An engineered bispecific DNA-encoded IgG antibody protects against *Pseudomonas aeruginosa* in a pneumonia challenge model. *Nat Commun*. 2017;8(1):637.
 18. Elliott STC, et al. DmAb inoculation of synthetic cross reactive antibodies protects against lethal influenza A and B infections. *NPJ Vaccines*. 2017;2(18):s41541-017-0020-x.
 19. Muthumani K, et al. Rapid and long-term immunity elicited by DNA-encoded antibody prophylaxis and DNA vaccination against chikungunya virus. *J Infect Dis*. 2016;214(3):369-378.
 20. Flingai S, et al. Protection against dengue disease by synthetic nucleic acid antibody prophylaxis/immunotherapy. *Sci Rep*. 2015;5:12616.
 21. Esquivel RN, et al. In vivo delivery of a DNA-encoded monoclonal antibody protects non-human primates against Zika virus. *Mol Ther*. 2019;27(5):974-985.
 22. deCamp A, et al. Global panel of HIV-1 Env reference strains for standardized assessments of vaccine-elicited neutralizing antibodies. *J Virol*. 2014;88(5):2489-2507.
 23. Sardesai NY, Weiner DB. Electroporation delivery of DNA vaccines: prospects for success. *Curr Opin Immunol*. 2011;23(3):421-429.
 24. Huang J, et al. Identification of a CD4-binding-site antibody to HIV that evolved near-pan neutralization breadth. *Immunity*. 2016;45(5):1108-1121.
 25. Scheid JF, et al. Sequence and structural convergence of broad and potent HIV antibodies that mimic CD4 binding. *Science*. 2011;333(6049):1633-1637.
 26. Gristick HB, et al. Natively glycosylated HIV-1 Env structure reveals new mode for antibody recognition of the CD4-binding site. *Nat Struct Mol Biol*. 2016;23(10):906-915.
 27. Walker LM, et al. Broad neutralization coverage of HIV by multiple highly potent antibodies. *Nature*. 2011;477(7365):466-470.
 28. Julg B, et al. Broadly neutralizing antibodies targeting the HIV-1 envelope V2 apex confer protection against a clade C SHIV challenge. *Sci Transl Med*. 2017;9(406):eaal1321.
 29. Gardner MR, et al. Anti-drug antibody responses impair prophylaxis mediated by AAV-delivered HIV-1 broadly neutralizing antibodies. *Mol Ther*. 2019;27(3):650-660.
 30. Kuriakose A, Chirmule N, Nair P. Immunogenicity of biotherapeutics: causes and association with posttranslational modifications. *J Immunol Res*. 2016;2016:1298473.
 31. Martinez-Navio JM, Fuchs SP, Pedreño-López S, Rakasz EG, Gao G, Desrosiers RC. Host anti-antibody responses following adeno-associated virus-mediated delivery of antibodies against HIV and SIV in rhesus monkeys. *Mol Ther*. 2016;24(1):76-86.
 32. Singh S, et al. Monoclonal antibodies: a review. *Curr Clin Pharmacol*. 2018;13(2):85-99.
 33. Sparrow E, Friede M, Sheikh M, Torvaldsen S. Therapeutic antibodies for infectious diseases. *Bull World Health Organ*. 2017;95(3):235-237.
 34. Welles HC, et al. Vectored delivery of anti-SIV envelope targeting mAb via AAV8 protects rhesus macaques from repeated limiting dose intrarectal swarm SIVsmE660 challenge. *PLoS Pathog*. 2018;14(12):e1007395.
 35. Julg B, et al. Protection against a mixed SHIV challenge by a broadly neutralizing antibody cocktail. *Sci Transl Med*. 2017;9(408):eaao4235.
 36. Moldt B, et al. Highly potent HIV-specific antibody neutralization in vitro translates into effective protection against mucosal SHIV challenge in vivo. *Proc Natl Acad Sci USA*. 2012;109(46):18921-18925.
 37. Shingai M, et al. Passive transfer of modest titers of potent and broadly neutralizing anti-HIV monoclonal antibodies block SHIV infection in macaques. *J Exp Med*. 2014;211(10):2061-2074.
 38. Barouch DH, et al. Therapeutic efficacy of potent neutralizing HIV-1-specific monoclonal antibodies in SHIV-infected rhesus monkeys. *Nature*. 2013;503(7475):224-228.
 39. Pardi N, et al. Administration of nucleoside-modified mRNA encoding broadly neutralizing antibody protects humanized mice from HIV-1 challenge. *Nat Commun*. 2017;8:14630.
 40. Badamchi-Zadeh A, et al. Therapeutic efficacy of vectored PGT121 gene delivery in HIV-1-infected humanized mice. *J Virol*. 2018;92(7):e01925-17.
 41. Khoshnejad M, et al. Development of novel DNA-encoded PCSK9 monoclonal antibodies as lipid-lowering therapeutics. *Mol Ther*. 2019;27(1):188-199.
 42. Kontermann RE. Strategies to extend plasma half-lives of recombinant antibodies. *BioDrugs*. 2009;23(2):93-109.
 43. Margolis DM, Koup RA, Ferrari G. HIV antibodies for treatment of HIV infection. *Immunol Rev*. 2017;275(1):313-323.
 44. Sarzotti-Kelsoe M, et al. Optimization and validation of the TZM-bl assay for standardized assessments of neutralizing antibodies against HIV-1. *J Immunol Methods*. 2014;409:131-146.
 45. Adachi A, et al. Production of acquired immunodeficiency syndrome-associated retrovirus in human and nonhuman cells transfected with an infectious molecular clone. *J Virol*. 1986;59(2):284-291.
 46. Pollara J, et al. High-throughput quantitative analysis of HIV-1 and SIV-specific ADCC-mediating antibody responses. *Cytometry A*. 2011;79(8):603-612.
 47. Pollara J, et al. HIV-1 vaccine-induced C1 and V2 Env-specific antibodies synergize for increased antiviral activities. *J Virol*. 2014;88(14):7715-7726.